Indian J. Phys. **66B** (3), 245-255 (1992)

Structure of explosion shocks in the central region of the Galaxy and their role on star formation

B Basu and Tanuka Kanjilal
Department of Applied Mathematics, Calcutta University, Calcutta-700 009, India

Received 19 November 1991, accepted 9 March 1992

Abstract : The structure of the compressed gas behind a plane steady shock generated as a result of nuclear explosion in the central region of the Galaxy has been computed. The temperature and density profiles are shown and the thickness of the different layers of the compressed region is calculated for different values of the parameters. The Jeans mass for gravitational collapse of the cold molecular layer accumulated behind the shock-front has been computed. It is found that for a lower initial density and comparatively weaker shocks formation of galactic clusters is more likely. On the other hand, the possibility of forming clusters behind strong shocks propagating through high density ambient gas can almost be ruled out.

Keywords : Nuclear explosion, shock propagation, Galaxy, Jeans mass, star formation.

PACS Nos. : 98.50 Lh, 97.10. Bt

1. Introduction

Different explosive phenomena occurring in the nucleus of our Galaxy are belived to trigger star formation in the central region. Strong shock waves are generated as the result of explosions. As these waves propagate through the ambient medium they heat and compress the gas behind them, which when cools down undergoes gravitational instability and fragments. These fragmented subunits are the molecular clouds. A large number of molecular cloud complexes surrounding the nucleus, has been detected by radio survey of CO by Bally *et al* (1987, 1988). The molecular rings observed at various distances from the centre of our Galaxy have been interpreted by many authors as the results of explosion shocks (Kato 1977, Saitō and Saitō 1977, Saitō and Deguchi 1980). Large Scale shocks associated with spiral density waves have been suggested to be the cause of formation of new generations of stars by many authors (Roberts 1969, Woodward 1976). Sequential formation of OB stars in cloud complexes by shocks generated as a result of supernova explosions has been considered by Elmegreen and Lada (1977). Bhattacharya and Basu (1982) and Saha *et al* (1985) studied the propagation of shocks produced by gigantic explosions and their influences on the star formation in the central region of the Galaxy. Basu and Kanjilal (1989) showed that high energy explosion can lead to star formation from

the first generation of fragmentation closer to the centre (50 parsecs) and cluster formation is favoured at somewhat larger distances.

In the present work we have considered the structure of the different layers of compressed gas behind a plane, steady shock generated as a result of nuclear explosion and have calculated the Jeans mass after gravitational collapse of the cooled molecular layer accumulated far behind the shock front. In Section 2 we have discussed about the temperature and density profiles and thicknesses, computed in the different layers of the compressed region behind the shock for different values of shock speeds and densities of the ambient medium. In Section 3, the rates of cooling in the different regions have been calculated. Also calculated in this section, is the thickness of the growing molecular layer furthest behind the shock as well as the Jeans mass for gravitational collapse in this cold, accumulated layer. The paper is concluded in Section 4.

2. Structure of the layers of gas behind a plane steady shock

Let us consider a gaseous medium at temperature T, pressure p and density ρ. Let L be the energy radiated by the gas per unit volume per second and G be the energy absorbed by the gas under the same condition. Then,

$$G - L = p \frac{d}{dt} \ln(T^{3/2}/\rho), \qquad \text{(Kaplan 1966)}$$

where $(G-L)$ is the effective cooling (or heating rate). If there is overall cooling we write $-\Lambda(\rho, T) = G - L$.

Then, $\Lambda(\rho, T) = -p \frac{d}{dt} \ln(T^{3/2}/\rho) \equiv -p \left[\frac{\partial}{\partial t} + (\vec{v} . \vec{\Delta}) \right] \ln (T^{3/2}/\rho)$, where $\vec{v}$ is the gas velocity.

For steady one-dimensional flow,

$$\Lambda(\rho, T) = -pv \frac{d}{dx} \ln(T^{3/2}/\rho).$$

If the co-ordinate system moves with the front at a constant velocity D, then the above equation has the form

$$\Lambda(\rho, T) = -p(D - v) \frac{d}{dx} \ln(T^{3/2}/\rho),$$

which can be written as,

$$dx = -p \frac{(D - v)}{\Lambda(\rho, T)} d \ln(T^{3/2}/\rho). \qquad (2.1)$$

Let us consider a strong shock generated by a nuclear explosion at the centre of a galaxy. This shock advances through the gaseous medium and we consider it to be steady when its velocity reduces to say, D.

Let p_1, ρ_1 and p, ρ be respectively the pressures and densities ahead of and behind the

front. The velocity of gas behind the shock front is v. Then the conservation equations for mass and momentum are,

$$\rho (D - v) = \rho_1 D, \tag{2.2}$$

$$\rho (D - v)^2 + p = \rho_1 D^2 + p_1 \tag{2.3}$$

The equation of state of the gas is

$$p = \frac{R\rho T}{\mu} \tag{2.4}$$

where R is the universal gas constant and μ is mean molecular weight. Then using (2.4) in (2.2) and (2.3) one gets

$$\frac{R\rho T}{\mu} = p_1 + \rho_1 D^2 \left(1 - \frac{\rho_1}{\rho}\right) \tag{2.5}$$

Now, using eq. (2.2) in (2.1) and integrating, we get

$$x(\rho) = -\frac{R}{\mu} \int_{\rho_2}^{\rho} \frac{T(\rho)}{\Lambda(\rho, T)} \rho_1 D \, d \ln(T^{3/2}/\rho), \tag{2.6}$$

where ρ_2 is the density of the medium at the rear of the region just behind the front where no radiation occurs, and

$$\rho_2 \quad \frac{(\gamma + 1)(D/C)^2}{(\gamma - 1)(D/C)^2 + 2\gamma} \rho_1 \qquad \text{(Kaplan 1966)} \tag{2.7}$$

γ being the ratio of specific heats and C the isothermal speed of sound. We have,

$$C^2 = \frac{p_1}{\rho_1}, \gamma = 5/3$$

because interstellar medium contains monatomic gases. Some diatomic gases, if present, do not change its value considerably from the value taken above.

Using $T(\rho)$ from (2.5), eq. (2.6) can be integrated numerically using Simpson's one third rule for numerical integration to obtain the density profile in the shock compressed region for different known forms of $\Lambda(\rho, T)$. The thickness of that region can also be computed.

We can divide the compressed region behind the shock-front into three distinct layers. (i) A region just behind the front where the equipartition of energy prevails between atoms and ions and no radiation takes place. The thickness of this region is so small that it can be considered as a region of discontinuity. Let T_2, ρ_2 be respectively the temperature and density at the rear part of this region. (ii) A radiative region where no chemical reaction occurs and cooling occurs by radiation of atoms or ions. (iii) A region where chemical reaction occurs leading to molecule formation and cooling takes place by atoms and molecules.

Let T_3, ρ_3 and T_4, ρ_4 be respectively the temperatures and densities of the shock-compressed gas at the rear of the region (ii) and that of the region (iii).

Let x_3 and x_4 be the mean distances of the farthest points in the regions (ii) and (iii) respectively behind the front measured with the origin on the front. Then $(x_4 - x_3)$ is the thickness of the molecular layer at an epoch. This is given in the last column of Table 1. Table 1 also contains the various results, numerically computed, for regions (i), (ii) and (iii).

The first column of Table 1, gives the values of shock speeds, propagating through the ambient medium. Columns second and third give respectively the temperature and density at the rear of region (i) where cooling has not yet started. Columns four and five give the corresponding values for the rear of region (ii) while column six shows the thickness of this region. Column seven shows the thickness of the region (iii). This thickness is quite small. As the shock propagates, the thickness of the molecular layer $(x_4 - x_3)$ at an epoch remains unchanged. But more gas is swept out by the front and the cold gas continually accumulates behind the region (iii) increasing continually the thickness of this layer with time. This is discussed in Section 3.

It is clear from Table 1 that with the increase of the shock strength both the temperature T_2 and thickness x_3 increase. For weaker shocks ($D \sim 100$ kms^{-1}) x_3 is always less than 1 parsec which is compatible with the result obtained by Pikel'ner (1954). For comparatively strong shock, the thickness increases upto 14 parsecs because for strong shocks the initial rise of temperature is high ($\geq 10^6$ K) while the initial compression is more or less the same (~ 4). Since the rate of cooling is proportional to the square of the density cooling is slow in the high temperature low density region. Also at very high temperature free-free emission is the only cooling process which slows down the rate of cooling.

Figures 1(a), 1(b) and 2(a), 2(b), show the temperature-density profiles in region (ii) and Figures 3(a) and 3(b) show those in region (iii) for different initial densities and for different shock speeds. The fall of temperature is rapid for $T \sim 10^4$ K because cooling occurs here by strong line emissions.

For 1000 K $< T < 10^4$ K the fall of temperature is rather slow. The ionization for this range is considered to be 10%. At these temperatures chemical reactions and formation of molecules may be considered as unimportant and may be ignored in this case. Cooling is therefore rather slow.

From Figures 3(a) and 3(b) it is clear that in the temperature range 100 K $< T <$ 1000 K, the cooling is very rapid because cooling by molecules is included here. Also efficient cooling renders the density of the medium quite high. Figure 3(a) also shows that with the increase of the shock speed the density rise is high in region (iii). Now, as the shock speed increases, the initial rise of temperature is high and this leads to sufficiently high density in growing molecular layer. Again, with the increase of density of the ambient medium, initial compression is high so the density rise in the molecular layer is also high. This is clearly indicated by Figure 3(b) when compared to Figure 3(a).

Table 1. The structure of shock-compressed layer for different values of the shock speeds and an initial density $\rho_1 = 20\text{H cm}^{-3}$ and temperature $T_1 = 100$ K of the ambient medium.

D (kms^{-1})	$(T_3/10^2)$ (o_k)	(ρ_3/ρ_1)	T_3 (o_k)	$(\rho_3/10^{-19})$ (gcm^{-3})	x_3 (parsec)	$(x_4 - x_3) / 10^8$ (cm)
100	2.94	4	753	5.3	5.73×10^{-3}	4.31
120	4.23	"	867	6.7	1.28×10^{-2}	4.56
140	5.76	"	984	8.0	2.73×10^{-2}	4.78
160	7.52	"	964	1.1	6.38×10^{-2}	4.78
180	9.51	"	976	1.3	1.42×10^{-1}	4.78
200	11.75	"	602	26.7	4.60×10^{-1}	4.04
220	14.21	"	729	26.7	8.27×10^{-1}	4.31
240	16.92	"	867	26.7	1.09	4.56
260	19.85	"	678	40.1	2.10	4.04
280	23.02	"	787	40.1	2.67	4.31
300	26.43	"	900	40.1	3.33	4.78
320	30.07	"	771	53.4	5.49	4.31
340	33.95	"	870	53.4	6.72	4.56
360	38.06	"	976	53.4	8.14	4.78
380	42.41	"	869	66.8	12.25	4.58
400	46.99	"	969	66.8	14.65	4.78

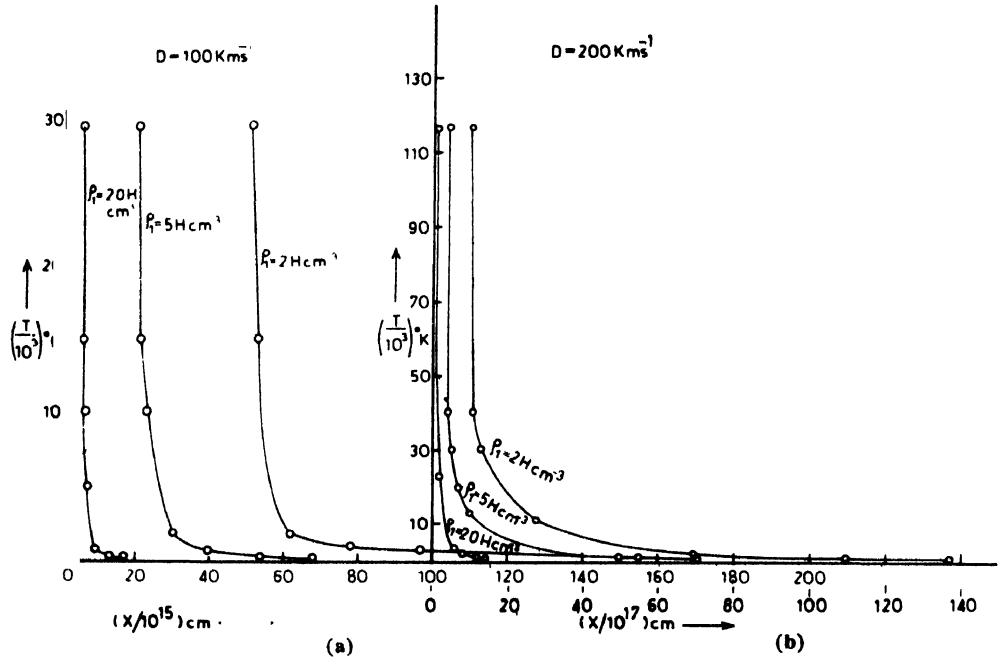

Figure 1. Temperature profiles in the radiative region (region, ii) for the densities 2H, 5H and 20H cm^{-3} respectively of the ambient medium at shock speed of (a) 100 kms^{-1} and (b) 200 kms^{-1}.

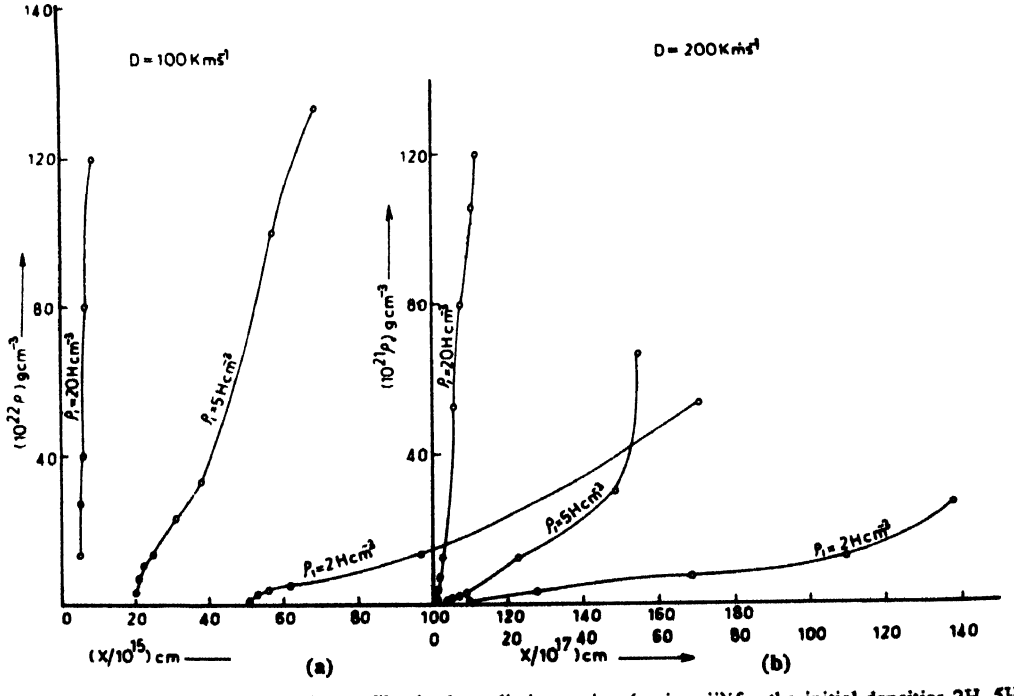

Figure 2. Density profiles in the radiative region (region, ii) for the initial densities 2H, 5H and 20H cm^{-3} respectively of the ambient medium at shock speed of (a) 100 kms^{-1} and (b) 200 kms^{-1}.

3. The rate of cooling for different regions behind the shock

(a) *The radiative region (region (ii)) :*

In order to determine $\Lambda(\rho, T)$ for the temperature range $10^4\ \mathrm{K} \leq T \leq 10^8\ \mathrm{K}$ in region (ii) we use the curve given by Cox and Tucker (1969) and fit algebric relations for different ranges of temperature. For temperature range $10^3\ \mathrm{K} < T < 10^4\ \mathrm{K}$ we use the cooling relation $[\Lambda(\rho, T), T]$ given by Kaplan (1966).

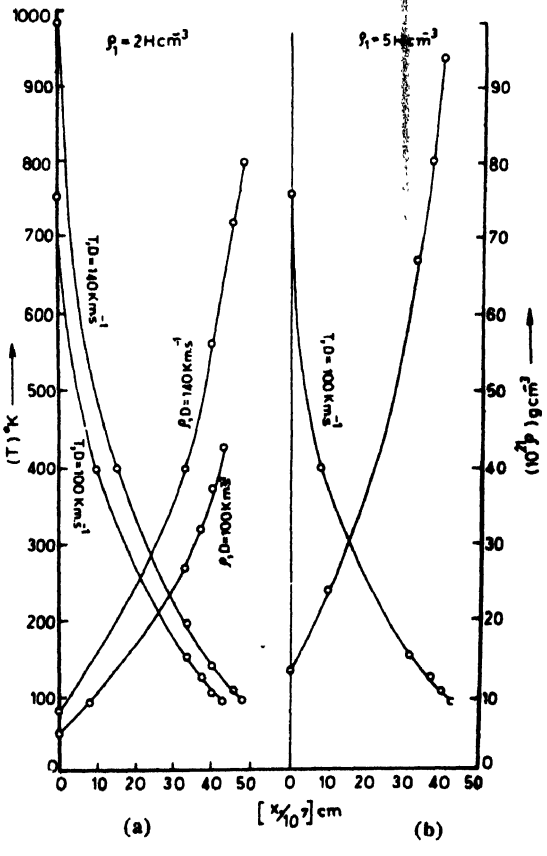

Figure 3. Density and temperature profiles in the molecular layer (region, iii) (a) at shock speed of 100 and 140 kms^{-1} and at an initial density $\rho_1 = 2\mathrm{H\ cm}^{-3}$ of the ambient medium, (b) at shock speed of 100 kms^{-1} and at an initial density $\rho_1 = 5\mathrm{H\ cm}^{-3}$ of the ambient medium.

In our computation we have considered 100% ionization for $T \geq 8 \times 10^5$ K, 50% ionization for $10^4\ \mathrm{K} \leq T < 8 \times 10^5$ K and 10% ionization for $T < 10^4$ K.

(b) *The molecular region (region (iii)) :*

In region (iii) cooling occurs mainly by atoms and molecules. We consider C, O and CO to be the major coolants. Then following Dalgarno and McCray (1972) and also Aannestad (1973)

Table 2. The structure of the molecular layer for different values of the shock speed and for an initial density $\rho_1 = 20\text{H cm}^{-3}$ of the ambient medium.

D (kms^{-1})	T (o_k)	($\rho_{4/10}$−18) (gcm^{-3})	($t_{ff}/10^4$) (yr)	$y(c)/10^{-6}$	$y(\text{O})/10^{-5}$	$y(\text{CO})/10^{-5}$	$y(\text{H})/10^{-5}$	$y(\text{H}_2)$	Thickness of the growing molecular layer (parsec)
100	94	4.3	10.20	7.81	6.25	3.24	3.89	0.4	10.71
120	96	6.0	8.59	7.74	6.21	3.27	3.85	0.4	10.84
140	98	8.0	7.44	7.66	6.17	3 31	3.31	0.4	10.95
160	96	10.7	6.44	7.55	6.10	3.36	3.75	0.4	10.83
180	98	13.3	5.76	7.44	6.04	3.41	3.68	0.4	10.90
200	86	18.7	4.87	7.23	5.92	3.51	3.55	0.4	10.24
220	91	21.4	4.55	7.12	5.86	3.56	3.49	0.4	10.53
240	96	24.0	4.29	7.01	5.80	3.61	3.43	0.4	10.83
260	97	28.0	3.98	6.85	5.70	3.69	3.33	0.4	10.87
280	98	32.1	3.72	6.69	5.61	3.77	3.24	0.4	10.95
300	90	40.1	3.33	6.36	5.43	3.92	3.05	0.4	10.49
320	96	42.7	3.22	6.26	5.37	3.97	2.98	0.4	10.83
340	98	48.1	3.04	6.04	5.24	4.07	2.85	0.4	10.85
360	98	53.4	2.88	5.83	5.12	4.17	2.73	0.4	10.9
380	97	60.1	2.72	5.56	4.97	4.30	2.57	0.4	10.85
400	96	66.8	2.58	5.29	4.81	4.42	3.20	0.4	10.83

$$\Lambda_o(\rho, T) = \{1.24\times10^{-24}\exp(-326/T) + 6.7\times10^{-24}\exp(-228/T)$$
$$\times [0.625 - 0.069\exp(-98/T)]\}\, T^{1/6} \qquad (3.1)$$
$$\times [n(\mathrm{H}) + n(\mathrm{H_2})/4]\, n(\mathrm{O}),$$

$$\Lambda_c(\rho, T) = \{2.2\times10^{-24}\exp(-63/T) + 4.48\times10^{-24}\exp(-24/T)$$
$$\times [0.25 - 0.14\exp(-39/T)]\}\, T^{1/6}\, [n(\mathrm{H}) + n(\mathrm{H_2})/4]\, n(\mathrm{C}) \qquad (3.2)$$

$$\Lambda_{co}(\rho, T) = 7\times10^{-26}\,[1 - (5.3/T)\exp(-T/20)]\, T^{1/2} \qquad (3.3)$$
$$\times \exp(-5.3/T)\, n(\mathrm{H_2})\, n(\mathrm{CO}).$$

where $n(x)$ is the number density of the species x.

Let $y(x) = \dfrac{n(x)}{n}$ where n is the nucleon number density.

Then $n(x) = y(x)\dfrac{\rho}{m_H}$, $y(x)$ being the relative abundance of the species x.

In order to express $y(x)$ as a function of σ we use the curves given by Figure 2 of Suzuki *et al* (1976) and fit algebric relations for different ranges of density. Then,

$$\Lambda(\rho, T) = \Lambda_c(\rho, T) + \Lambda_{co}(\rho, T) + \Lambda_o(\rho, T) \qquad (3.4)$$

Using (3.4) in (2.6) the thickness of the molecular layer within which the temperature falls from 1000 K to 100 K has been computed. This is given in last column of Table 1.

Now, as the shock propagates with a speed D, more and more gas is swept out by the advancing front and the cold gas continually accumulates behind the region (iii). Thus the region (iii) grows in thickness almost at a speed at which the front propagates. We take T_4 and ρ_4 as the temperature and density of the growing molecular layer. We assume that the layer grows in thickness during a period equal to the free-fall time, $t_{ff} = \left(\dfrac{3\pi}{32G\rho}\right)^{1/2}$ for that layer.

So the thickness of the molecular layer formed within this time is $\sim D.t_{ff}$.

Table 2, gives the numerical results for the molecular layer for a density value $\rho_1 = 20$ H cm^{-3} of the ambient medium. In Table 2, columns 1, 2 and 3 represent respectively the velocities of the steady shock, the temperatures and the densities at the rear of the region (iii). Column 4 represents the free fall-times of the layer having density ρ_4. We have adopted the curves from Figure 2 of Suzuki *et al* (1976) showing the relative abundance $y(x)$ for the species x vs number density n and computed the relative abundances of various atoms and molecules corresponding to the density ρ_4 of the growing molecular layer in our case. Columns five to nine of Table 2 show these computed relative abundances. Column 10 gives the thicknesses of the molecular layer grown during the free-fall time.

The table shows that in every case the abundance of CO increases with the increase of the shock strength. The observation of CO molecules in large amount in molecular

clouds in the central region (Bally *et al* 1987, 1988) is consistent with our calculations. The thickness of the molecular layer is roughly 10 parsecs if the medium initially has a density of 20 H cm^{-3} The thickness increases with the decrease of initial density of the ambient medium. e.g., at ρ_1 = 2 H cm^{-3} the thickness is roughly 34 parsecs, at ρ_1 = 5 H cm^{-3} it is roughly 21 parsecs, while at ρ_1 = 10 H cm^{-3} it is roughly 15 parsecs.

The thickness does not depend much upon the shock-strength, because the chemical reactions occur at low temperatures which are practically independent of the initial temperatures.

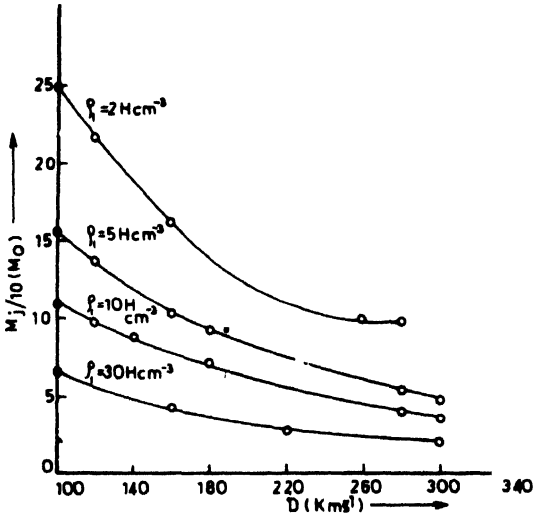

Figure 4. The Jeans mass for gravitation collapse (Mj), at different shock speeds (D) for ρ_1 = 2H, 5H, 10H and 30H cm^{-3} respectively of the ambient medium.

It is clear from Figure 4 that more and more strong shocks give rise to smaller and smaller Jeans mass irrespective of the density of the ambient medium. The figure also suggests that fragments of masses comparable to the galactic cluster masses will prevail more easily when both the ambient gas density and shock velocity are lower. As the values of the latter quantities increase the formation of fragments of galactic cluster masses become more and more difficult.

4. Conclusions

The principal conclusions drawn from our present work are as follows :

(i) The fall of temperature in the radiative region behind the shock is very rapid for $T \sim 10^4$ K because cooling occurs by strong line emissions around this temperature. For comparatively stronger shocks, where the initial rise of temperature is of the order of 10^6 K, the cooling is rather slow, because free emission is the only cooling process in this case which slows down the rate of cooling. So the thickness of the region (ii) is larger for a stronger shock than that for a weaker one.

(ii) For temperatures in the range 1000 K < T < 10^4 K, the fall of temperature is rather slow. No chemical reactions occur at such high temperatures. So cooling by molecules is not considered in this case. The cooling rate is slow here.

(iii) For the range of temperature 100 K < T < 1000 K, the cooling is very rapid, because molecules form at these temperatures and contributions by both atoms and molecules lead to very rapid cooling.

(iv) With the increase of the shock speed the density rise in the molecular layer in high and the CO abundance increases.

(v) The thickness of the growing molecular layer is practically independent of the shock speeds but increases with the decrease of the initial density of the ambient medium.

(vi) Formation of galactic clusters in the growing molecular layer is possible for a lower initial density of the ambient medium as well as for weaker shocks. But with the increase of the initial density (~ 30 H cm^{-3}) the formation of star cluster is unlikely. For stronger shocks the effect is more pronounced.

Acknowledgment

One of the authors (Tanuka Kanjilal) is very much thankful to the Council of Scientific and Industrial Research for awarding her a Senior research fellowship for the work.

References

Aannestad P A 1973 *Astrophys. J. Suppl. Ser.* **25** 223
Bally J, Stark A A, Wilson W and Henkel C 1987 *Astrophys. J. Suppl. Ser.* **65** 13
— 1988 *Astrophys. J.* **324** 223
Basu B and Kajilal T 1989 *Astrophys. Space Sci.* **152** 203
Bhattacharyya Tara and Basu B 1982 *Astrophys. Space Sci.* **83** 15
Cox D P and Tucker W H 1969 *Astrophys. J.* **157** 1157
Dalgarno A and McCray R A 1972 *Ann. Rev. Astron. Astrophys.* **10** 375
Elmegreen B G and Lada J L 1977 *Astrophys. J.* **214** 725
Kaplan S A 1966 *Interstellar Gas Dynamics* F D Kahn (ed.) (Oxford : Pergamon) p 26, p 43
Katō T 1977 *Publ. Astron. Soc. Japan* **29** 369
Pikelner S B 1954 *Izv. Krymsk Observ.* **12** 94
Roberts W W 1969 *Astrophys. J.* **158** 123
Saha Anuradha, Basu B and Bhattacharyya Tara 1985 *Astrophys. Space Sci.* **116** 313
Saitō Mamoru and Deguchi Shuji 1980 *Publ. Astron. Soc. Japan* **32** 257
Saitō Mamoru and Saitō Yasumichi 1977 *Publ. Astron. Soc. Japan* **29** 387
Suzuki H, Miki S, Satō K, Kiguchi M and Nakagawa Y 1976 *Prog. Theor Phys* **56** 1111
Woodward P R 1976 *Astrophys. J.* **207** 484